# Conversion of heat to light using Townes' maser-laser engine: Quantum optics and thermodynamic analysis

C. H. Raymond Ooi*
*Department of Physics, University of Malaya, 50603 Kuala Lumpur, Malaysia*
(Received 2 December 2010; published 29 April 2011)

It is shown that thermal energy from a heat source can be converted to useful work in the form of maser-laser light by using a combination of a Stern-Gerlach device and stimulated emissions of excited particles in a maser-laser cavity. We analyze the populations of atoms or quantum dots exiting the cavity, the photon statistics, and the internal entropy as a function of atomic transit time, using the quantum theory of masers and lasers. The power of the laser light is estimated to be sufficiently high for device applications. The thermodynamics of the heat converter is analyzed as a heat engine operating between two reservoirs of different temperature but is generalized to include the change of internal quantum states. The von Neumann entropies for the internal degree are obtained. The sum of the internal and external entropies increases after each cycle and the second law is not violated, even if the photon entropy due to finite photon number distribution is not included. An expression for efficiency relating to the Carnot efficiency is obtained. We resolve the subtle paradox on the reduction of the internal entropy with regards to the path separation after the Stern-Gerlach device.

DOI: 10.1103/PhysRevA.83.043838 PACS number(s): 42.50.Pq, 07.20.Pe, 89.70.Cf

## I. INTRODUCTION

The second law of thermodynamics asserts that heat cannot be converted completely to work [1]. Its connection to entropy and extension to the quantum regime has been the subject of extensive discussions at a recent meeting [2]. In statistical thermodynamics the law ensures that matter cannot be cooled in a cyclic process without a dissipative mechanism [3]. According to Lloyd [4,5], the second law is not violated when information or knowledge is involved to realize an intelligent control mechanism called *Maxwell's demon*. The source of the intelligence lies in having information of a physical process, either via *prior knowledge* through predictability or measurement. The knowledge can be used to control and reduce the entropy of a subsystem. In other words, intelligence can be used to restore order from disorder since entropy is associated with disorder. However, there is a cost in acquiring the intelligence, which we refer to as "setup" entropy, which accounts, effectively, to the increase in the total entropy. It is possible to establish a system of negative entropy [6,7] that can be used to reduce the entropy of another system or subsystem [8] even if the process is not in equilibrium, is not closed, or does not evolve in cycles.

A Stern-Gerlach (SG) [9] device can be viewed as a kind of intelligent setup that inherits human knowledge in physics. A magnetic SG device works for particles with a permanent magnetic moment in a magnetic field through the Zeeman shift. Electrical SG devices work for particles with a permanent electric dipole moment in an electric field through the Stark effect. There is also an optical SG device but the quantum dynamics of these SG devices is essentially unitary. Townes and co-workers used the SG effect to make a focuser in the earlier construction of an ammonia maser [10,11]. This concept is so simple and ubiquitous that its potentiality for harnessing useful energy as laser light from ambient heat has been overlooked. A chapter in Feynman's lecture series [12] describes the atomic dynamics of the ammonia maser and estimates the spectral density of the maser field using the Schrödinger equation, but it does not consider the field damping through the maser cavity. The Townes' maser-laser setup forms a simple part of Scully's quantum afterburner Otto engine [13] where both maser and laser actions in three-level systems operate in tandem, but it does not involve thermodynamical processes of gas compression and expansion. The engine was shown to produce Carnot efficiency by using a two-level system [14].

In this paper, we show that energy from a heat source or reservoir can be converted into useful work in the form of photon energy or laser light. We propose a general scheme or setup composed of the SG device, quantum particles, and a maser-laser cavity [Fig. 1(a)]. The working fluid is quantum particles (more practically atomic gas or quantum dots) initially in equilibrium with a thermal heat source. The thermodynamics of the scheme can be understood by the standard heat flow diagram with two temperature reservoirs [see Fig. 1(b)] and does not violate the second law. The SG device separates the particles (ideally a two-level system) into different trajectories according to the *internal* (electronic, spin, vibrational, or rotational) quantum states, and they are guided through hollow tubes. The excited particles interact with the maser-laser cavity field where stimulated emissions produce maser-laser photons. The deexcited ensembles exiting from the maser-laser cavity are combined with an ensemble in the ground state and are ready to be thermalized [15] with the heat sink from the *external* degree (center-of-mass translational motion) for the next cycle operation. This may be realized by confining atomic gas or quantum dots inside tubes with spin-preserving coating. Our analysis is focused on the lasing mechanism, energy, entropy, and efficiency aspects using quantum optics and quantum thermodynamics.

Section II elaborates on the physical mechanisms of the SG process and the quantum optics of the field amplification in the maser-laser cavity. The results are used in Sec. III to

*rooi@um.edu.my

 

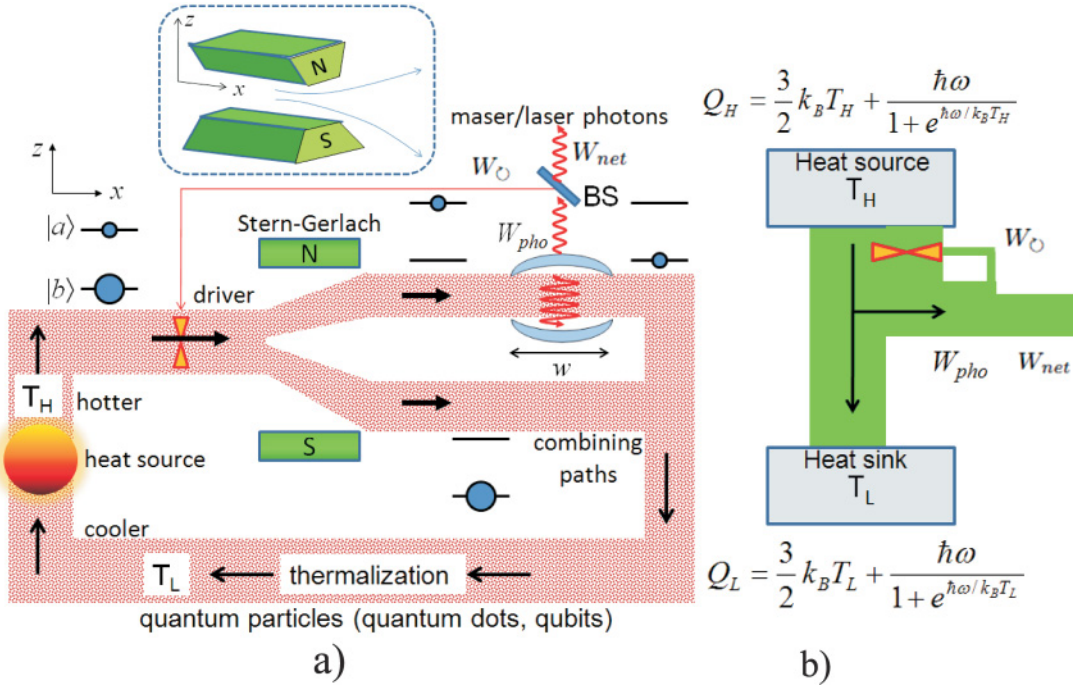


FIG. 1. (Color online) (a) A quantum heat converter converts heat into light using a Stern-Gerlach device, a maser-laser cavity, and a working fluid of quantum particles in a guiding tube. BS is the beam splitter. (b) Thermodynamic equivalence with two reservoirs, with the heat source at a higher temperature $T_H$ and the heat sink at a lower temperature $T_L$.

estimate the laser power output and efficiency. In Sec. IV, we elaborate on the thermodynamics of the system as a heat engine based on analysis of the energy balance. In Sec. V, we show how the internal entropies in the processes should be calculated, leading to the resolution of the paradox that the internal entropy decreases. In Sec. VI, we analyze the internal entropy change and the thermodynamic entropy change for the external degree to show that the second law is satisfied. Encouraging conclusions are given in Sec. VII based on the results.

## II. MECHANISMS IN THE QUANTUM HEAT CONVERTER

We analyze the physical mechanisms in the SG device and maser-laser cavity from the perspectives of quantum optics and consider practical aspects with realistic parameters.

### A. Stern-Gerlach separation

The SG [9] device is composed of dipolar magnets, with north and south poles aligned along the $z$ axis (see inset of Fig. 1). The $x$ dimension of the magnets should be long enough to provide significant angular deflection. The separation of the particles is based on conservative magnetic force, which introduces net momenta along the $z$ direction for the upper and lower ensembles, resulting in a slightly higher mean kinetic energy of the two ensembles. The particle beam (or fluid) flows from the thermal bath through the channel of a guiding tube and is in thermal equilibrium, which means that the particles move under the force of the SG device and are not affected by the pressure of neighboring particles. Note that the quantum particles or fluid cannot sustain a continuous flow without an energy supply. Thus, the particles have to be driven to move in one direction (as shown by the arrows in Fig. 1) by a driver which is powered by some energy $W_{\circlearrowleft}$ taken from the laser light.

For a molecular beam, a number of internal rotational levels are populated even though the levels are typically in the ground vibrational state at room temperature. Molecules in a rotational level $J$ would be deflected by the SG device into $2J + 1$ trajectories, each corresponding to a Zeeman substate. After leaving the magnetic field region, these molecules have essentially the same internal energy and can be combined in the same cavity tuned to the lasing transition. However, the molecules are distributed over several rotational levels, each requiring a distinctly tuned maser cavity which would produce lasing photons with different wavelengths, as illustrated in Fig. 2(a). For vibrationally or electronically excited molecules from a hot reservoir, the situation becomes more complicated and requires a more elaborate experimental setup [16]. Thus, it is preferable (but not necessary) to use the working fluid composed of quantum particles with only the few lowest internal levels populated, such as an atomic gas or quantum dots (QD).

### B. Field amplification in the cavity

The dynamics and quantum statistics of photons inside the maser-laser cavity can be described by the quantum theory of masers and lasers [17,18]. The situation with continuously injected dots is identical to the quantum dot laser [19]. We identify the criteria for obtaining a large number of maser-laser photons by analyzing the photon number distribution and the populations of the particles exiting from the cavity.

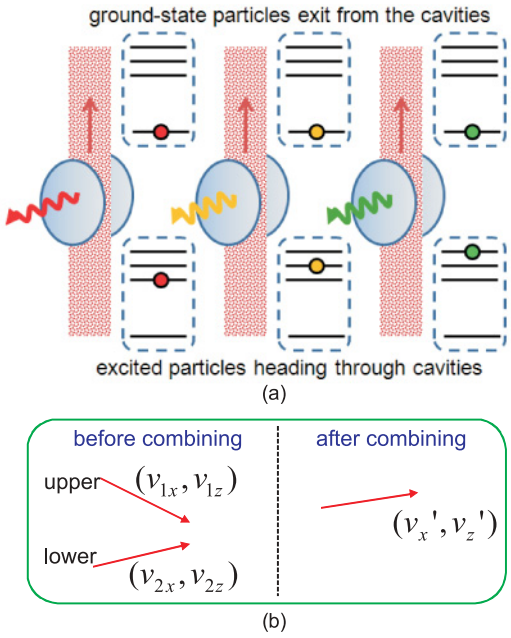


FIG. 2. (Color online) (a) Multipath excited ensembles are fed into maser-laser cavities, which generate a spectrum of maser or laser photons. (b) Velocity components of particles in the upper path and lower path before combining, and the components after combining.

### 1. Maser process

For the maser, the lasing wavelength is of the order of the width $w \sim 1$ cm of the microcavity. For particles with mean velocity $\bar{v} \gtrsim 50$ m s$^{-1}$, the average transit time through the cavity is $\tau = w/\bar{v}$, which is typically smaller than $1/\gamma_\mu \sim 10^{-2}$ s, the spontaneous lifetime of the microwave transition in ammonia molecules. For each particle entering the cavity, the decay is negligible and the amplified field in the cavity flips the excited particle to the lower state and back to the upper state repeatedly until the particle leaves the cavity. The rate of oscillations is the effective Rabi frequency [12] $g\sqrt{n+(\frac{\Delta}{2g})^2+1}$, which depends on the photon number $n$ and the detuning $\Delta = \nu - \omega - kv$, where $v$ is the transverse velocity of the particle beam and $k$ is the lasing photon wave vector. By using a highly collimated particle guide, the Doppler shift $kv$ would be negligible. The dynamics of the photon number distribution is governed by the master equation [17]

$$\frac{dp_n}{dt} = X_n p_{n-1} + Y_{n+1} p_{n+1} - (X_{n+1} + Y_n) p_n, \tag{1}$$

with

$$X_n = r \sin^2(g\tau\sqrt{n}) + \mathcal{C}n\bar{n}_{th}, \tag{2}$$

$$Y_n = \mathcal{C}n(\bar{n}_{th} + 1), \tag{3}$$

where $g$ is the particle-field coupling strength, $\mathcal{C}$ is the cavity damping rate, $\bar{n}_{th} = (e^{\hbar\nu/k_B T_a} - 1)^{-1}$ is the mean thermal photon number at ambient temperature $T_a$, and $r$ is the particle injection rate. The excited population of an exiting particle as a function of the transit time $\tau$ is found by tracing out the photon number,

$$\rho_{aa}^{(m)}(\tau) = \sum_n \rho_{an,an}(\tau) = \sum_n p_n^{(m)} \cos^2(g\tau\sqrt{n+1}), \tag{4}$$

with the steady-state diagonal density matrix element $\rho_{nn}$ of the maser master equation being the photon number distribution

$$p_n^{(m)} = p_0 \left(\frac{\bar{n}_{th}}{\bar{n}_{th}+1}\right)^n \prod_{k=1}^{n} \left(\frac{r_a \sin^2(g\tau\sqrt{k})}{\mathcal{C}\bar{n}_{th}k} + 1\right), \tag{5}$$

where $p_0$ is the normalization constant. We have used $\rho_{an,an}(\tau) = |C_{an}(\tau)|^2$ with $C_{an}(\tau) = C_n(0)\cos(\alpha_n\tau)$ as the coefficient of the state $|a,n\rangle$, $\rho_{nn} = p_n = |C_n(0)|^2$, and $\alpha_n = g\sqrt{n+1}$ since initially the particles are in level $a$. In the micromaser, the atomic decay rate is neglected since it is much smaller than the dynamic rate.

One might expect that the peaks of the maser correspond to the condition $\sin(g\tau\sqrt{\langle n\rangle}) = \pm 1$, or $g\tau\sqrt{\langle n\rangle} = \frac{2m+1}{2}\pi$, which maximizes $p_n^{(m)}$. In steady state, the mean number of photons loss through the cavity is $\langle n\rangle\mathcal{C}$, which is compensated by the rate $r$ of particles injected into the cavity, giving a crude estimate of the mean photon number $\langle n\rangle \simeq r/\mathcal{C}$. Thus, the peaks are expected at $g\tau = \frac{2m+1}{2}\pi/\sqrt{r/\mathcal{C}}$ with $m$ as integers. Figure 3(a) shows that the peak with the largest photon number, i.e., $\langle n\rangle = r/\mathcal{C} = 200$, occurs at around $\Theta = g\tau\sqrt{r/\mathcal{C}} = \frac{\pi}{2}$ or $g\tau\sqrt{\langle n\rangle} = \frac{\pi}{2}$. This point [red arrows in Figs. 3(a) and 3(b)] corresponds to all particles exiting in the lower level $b$ [$\rho_{aa}(\tau) \simeq 0$, i.e., the population is essentially in a single internal state] corresponding to a minimum internal entropy ($S/k_B = -\sum_{i=a,b} p_i \ln p_i = \ln 1$ is zero) and a maximum mean photon number $\langle n\rangle_{\max} = r/\mathcal{C} = 200$ [see Fig. 3(c)]. However, for higher transit times, the peak makes a transition (jump) from a lower to a higher mean photon number at every $1.5\pi$ interval, i.e., $\Theta \simeq 2\pi, 3.5\pi, 5\pi$. Note that this does not satisfy $\Theta = g\tau\sqrt{r/\mathcal{C}} = \frac{2m+1}{2}\pi$. Instead, it satisfies $g\tau\sqrt{\langle n\rangle} = \frac{2m+1}{2}\pi$ with $\langle n\rangle \leqslant r/\mathcal{C}$. Then $\rho_{aa}^{(m)}$ oscillates with $\Theta$ [Fig. 3(b)] in a nonsinusoidal fashion, with an abrupt drop around a transition point due to the jump of the peak to a higher photon number [refer to Fig. 3(a)]. For large transit times, the oscillations in $\rho_{aa}^{(m)}$ disappear and the particles exit essentially with equal probability in levels $a$ and $b$ [i.e., $\rho_{aa}(\infty) \to 0.5$], with a constant entropy of $S_{\rm cav}^u/k_B \to \ln 2 \simeq 0.69$. Thus, the particles exiting the maser cavity are not necessarily in the lower level $b$. If a smaller $r/\mathcal{C}$ is used, there would be collapse and revival in the oscillations.

Although the Rabi oscillations contribute to the internal particle dynamics, there are no simple analytical expressions for $\rho_{aa}^{(m)}(\tau)$ and $\rho_{bb}^{(m)}(\tau)$. The simulations provide clues to obtain the particular transit times ($\propto \Theta$) that maximize the number of particles exiting in the lower state. This enables us to maximize the number of photons in the cavity. Thus, precise control of the mean velocity $\bar{v}$ of the particles and the cavity width $w$ is important to obtain the desired $\tau = w/\bar{v}$. This is supplemented by adjusting the parameters, $g$, $r_a$, and $\mathcal{C}$ such that $p_n$ has peak(s) around large values of $n$ to produce an intense maser field.

### 2. Laser process

In the optical regime, the internal transitions of the particles due to spontaneous emissions and Rabi flopping occur on a time scale of $\sim 10^{-8}$ s, much shorter than the particle transit time. According to the quantum theory of lasers [18], the laser field and the photon statistics vary noticeably within a time

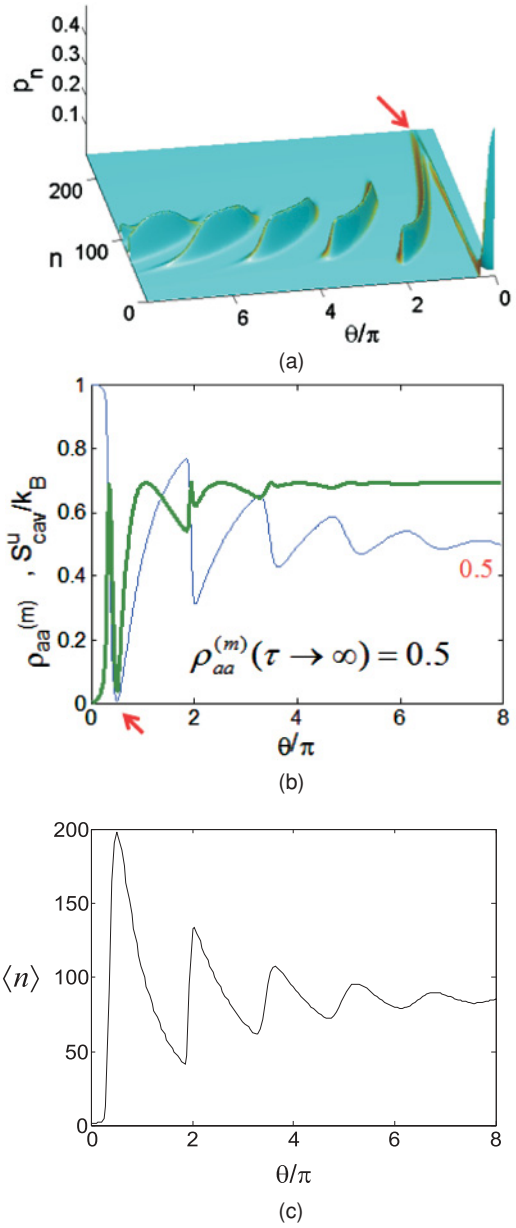


FIG. 3. (Color online) (a) Steady-state photon statistics of a maser vs $\Theta = g\tau\sqrt{r/\mathcal{C}}$, the dimensionless parameter for transit time $\tau$. (b) Population of level $a$ and the corresponding internal entropy (thick line) of exiting atoms. (c) Mean photon number generated in the cavity. Note that the nonsinusoidal oscillations across $\tau$ indicate the influence of multipeak photon number distribution and the Rabi oscillations in the atomic dynamics. Here, we use $\bar{n}_{th} = 1$, $\gamma = 10^8\ \mathrm{s}^{-1}$, $g = \gamma$, and $r/\mathcal{C} = 200$.

scale much longer than the decay lifetime $\gamma^{-1}$ such that we can add up the laser fields contributed by all particles in the cavity, each with different injection times [20], for example, $\int_0^\infty \gamma|C_{an}(\tau)|^2 d\tau = \int_0^\infty \gamma e^{-\gamma\tau}\cos^2(\alpha_n\tau)d\tau = \frac{\gamma^2+2\alpha_n^2}{\gamma^2+4\alpha_n^2}$. Thus, the resulting photon statistics would not depend on the duration of the transit time $\tau$. The theory successfully describes the photon statistics of lasers as the result of stimulated emission and cavity amplification mechanisms, in addition to the statistical contribution of many particles.

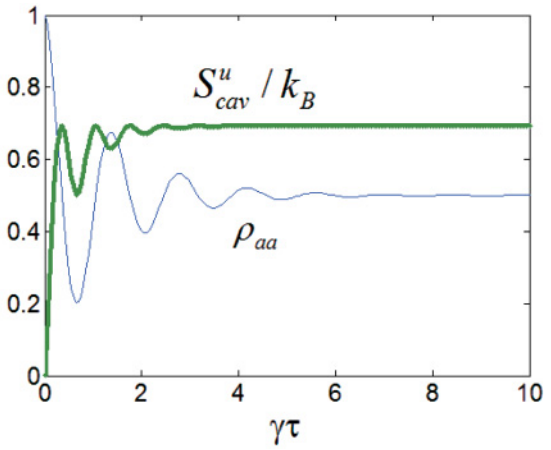


FIG. 4. (Color online) Population (thin line) $\rho_{aa}(\tau)$ [based on Eq. (6)] of an atom exiting the cavity in level $a$ and the corresponding internal entropy $S^u_{\mathrm{cav}}(\tau)$ (thick line) as a function of transit time $\tau$ showing the damping of the oscillations with mean photon number $\langle n\rangle = 2000$. We use $r/\mathcal{C} = 450$, $\gamma = 10^8\ \mathrm{s}^{-1}$, and $g = 0.1\gamma$.

The dynamics of an atom in the laser cavity can be obtained from the theory of resonance fluorescence driven by the quantized laser field. The matrix element $\rho_{an,an}(\tau) = \rho_{nn}\frac{1}{2}[1 + e^{-3\gamma\tau/4}\cos(g\tau\sqrt{n+1})]$ now includes the exponential term that was set to unity in the maser case. The population of an exiting particle as a function of the transit time $\tau$ is obtained by tracing out the photon number,

$$\rho_{aa}(\tau) = \sum_n p_n \frac{1}{2}[1 + e^{-3\gamma\tau/4}\cos(g\tau\sqrt{n+1})], \qquad (6)$$

with the exact steady-state photon number distribution,

$$p_n = \frac{p_0}{(\bar{n}_{th}+1)}\prod_{k=1}^{n}\left(\frac{\mathcal{A}/\mathcal{C}}{1+k\frac{\mathcal{B}}{\mathcal{A}}}\right), \qquad (7)$$

where $\mathcal{A} = r\frac{2g^2}{\gamma^2}$ and $\mathcal{B} = \frac{4g^2}{\gamma^2}\mathcal{A}$. Note that the laser photon statistics does not depend on the transit time, unlike the maser case.

For comparison with the maser case, we plot Eq. (6) in Fig. 4, which shows that the oscillations of the excited population for the exiting particles disappear for long transit times and the particles end up equally in both upper and lower levels: $\rho_{aa}(\infty) \simeq \rho_{bb}(\infty) \to 0.5$. Thus, we expect that the maser and laser have the same efficiency, which is 50%. The particles exiting the laser cavity after a long transit have a corresponding internal entropy of $S^u_{\mathrm{cav}}/k_B \to \ln 2$, as in the maser case. The mean photon number $\langle n\rangle = \sum_n np_n$ is independent of the transit time. So, it is compatible with the population $\rho_{aa}(\tau)$ at transit times greater than a few $1/\gamma$ or the coarse graining time.

### C. Combining the paths

Previous work shows that an information entropy of $k_B \ln 2$ has to be spent to coherently combine two wave packets of particles without heating up the system [21]. Instead of using information to coherently combine the particles from the upper and lower arms, here, we are dealing with a realistic situation composed of a continuous flow of ensembles

of particles, where no synchronization of wave packets is possible. When the ensemble of particles in the upper and lower paths are combined, collisions between the particles reduce the transverse mean momenta close to zero, while reducing the overall kinetic energy and increasing the width of the momentum distribution.

Let us consider the kinematics in Fig. 2(b) in order to understand how the external (center-of-mass) entropy (associated with the momentum width of the particles) can increase as the result of the incoherent combination without invoking information. The conservation of both the $x$- and $z$-component momenta before and after the collision gives $v'_{1x}+v'_{2x}=v_{1x}+v_{2x}$ and $v'_{1z}+v'_{2z}=v_{1z}-v_{2z}$, respectively. Energy conservation gives $2v=\sqrt{v_1'^2+v_2'^2}=\sqrt{v_{1x}'^2+v_{2x}'^2+v_{1z}'^2+v_{2z}'^2}$. If the particles move almost entirely along the $x$ direction, $v$ would range between $\frac{1}{2}\sqrt{2(v_{1x}+v_{2x})^2}=\sqrt{2}\frac{(v_{1x}+v_{2x})}{2}$ when $v'_1=v'_2=v_{1x}+v_{2x}$ and $\frac{1}{2}\sqrt{2\frac{1}{4}(v_{1x}+v_{2x})^2}=\frac{v_{1x}+v_{2x}}{2\sqrt{2}}$ when $2v'_1=2v'_2=v_{1x}+v_{2x}$. The velocity distribution is broadened from $\frac{\bar{v}}{\sqrt{2}}$ to $\sqrt{2}\bar{v}$, where $\bar{v}$ is the mean velocity of both ensembles. Inelastic collisions between the molecules will eventually make the center-of-mass (external) temperature equal to the internal temperature, establishing thermalization and creating some entropy.

## III. LASER POWER OUTPUT

Here, we consider the power aspect for the laser case. We use the results from the quantum theory of lasers and the lasing condition for estimating the power of laser light. The phase dynamics of the field is described by the photon number coherences in the off-diagonal density matrix element $\rho_{mn}$ $(m\neq n)$. For operation far above threshold ($\mathcal{A}/\mathcal{C}\gg 1$, good cavity, and large particle injection rate) the matrix element gives the normalized [$\int f(\nu)d\nu=1$] Lorentzian laser linewidth,

$$f(\nu)=\frac{D/\pi}{(\nu-\omega)^2+D^2}, \tag{8}$$

where the linewidth is $D\simeq\frac{\mathcal{A}+\mathcal{C}}{\bar{n}}=\frac{\mathcal{BC}}{\mathcal{A}}\frac{\mathcal{A}+\mathcal{C}}{\mathcal{A}-\mathcal{C}}\simeq\frac{\mathcal{BC}^2}{\mathcal{A}^2}$. The mean photon number in the laser cavity can be obtained from $\langle n\rangle=\sum_{n=1}^{\infty}np_n$ and has the analytical expression

$$\langle n\rangle=\frac{\mathcal{A}}{\mathcal{C}}\left(\frac{\mathcal{A}-\mathcal{C}}{\mathcal{B}}\right)=\frac{2rg^2/\mathcal{C}\gamma^2-1}{4g^2/\gamma^2}=\frac{r}{2\mathcal{C}}-\left(\frac{\gamma}{2g}\right)^2. \tag{9}$$

When the injection rate exceeds the threshold, $r>\mathcal{C}\gamma^2/2g^2$ or $\mathcal{A}>\mathcal{C}$, we obtain $\langle n\rangle\simeq\frac{r}{2\mathcal{C}}=\frac{\mathcal{A}^2}{\mathcal{BC}}\simeq\frac{\mathcal{C}}{D}$.

For large pumping or injection rate, $\frac{\mathcal{B}}{\mathcal{A}}\gg 1$, we have $\frac{\mathcal{A}/\mathcal{C}}{1+k\frac{\mathcal{B}}{\mathcal{A}}}\to\frac{1}{k}\frac{\mathcal{A}^2}{\mathcal{BC}}=\frac{1}{k}\langle n\rangle_c$. Replacing $\prod_{k=1}^{n}\frac{\langle n\rangle_c}{k}=\frac{\langle n\rangle_c^n}{n!}$ in the exact expression for $p_n$ [Eq. (7)] gives the coherent state with a Poissonian distribution

$$p_n=\frac{1}{n!}\langle n\rangle_c^n e^{-\langle n\rangle_c} \tag{10}$$

with the mean photon number related to the linewidth, i.e., $\langle n\rangle_c=\frac{\mathcal{A}^2}{\mathcal{BC}}\simeq\mathcal{C}/D$.

The power output of the laser is the number of photons dissipated, $\mathcal{C}\langle n\rangle$, multiplied by the photon energy averaged over the laser linewidth,

$$P=\mathcal{C}\langle n\rangle\int\hbar\nu f(\nu)\,d\nu. \tag{11}$$

The integral gives $\hbar\frac{D}{\pi}\int_0^{\infty}\frac{\nu}{(\nu-\omega)^2+D^2}d\nu=\hbar\frac{D}{\pi}\int_{-\infty}^{\infty}\frac{xdx}{x^2+D^2}+\hbar\omega=\hbar\omega$. When the injection rate exceeds the threshold, we have

$$P\approx\frac{r}{2}\hbar\omega. \tag{12}$$

The factor $1/2$ in Eq. (12) arises because the quantum theory of lasers gives the result for large $\tau$, such that only 50% of the input (excited) population converts the internal energy into photon energy. In general, we may replace $1/2$ by $\rho_{aa}(\tau)$ and write $P=r\rho_{bb}(\tau)\hbar\omega$. Using $\gamma\sim 10^8$, $g\sim 10^6$, $r\sim 10^{15}$ s$^{-1}$, $\mathcal{A}\sim 2\times 10^{10}$, $\mathcal{B}=\frac{4}{10^4}\mathcal{A}$, and $\mathcal{C}\sim 0.01\mathcal{A}$, we find a moderate power $P\sim 50$ $\mu$W.

The rate of the excited particle beam passing through the cavity can be expressed as

$$r=dN_c/dt\simeq N_c/\tau=\rho A\bar{v}=N_c\bar{v}/L, \tag{13}$$

where $\bar{v}=dl/dt$ is the mean velocity, $\rho=N_c/V$ is the number density, and $A$ is the cross section of the beam of particles. The number of excited particles in the cavity of length $L$ is $N_c=\rho AL$.

The typical gas number density at room temperature is $\rho\sim 10^{25}$ m$^{-3}$. For a particle beam with a radius of 5 mm, $A=\pi 0.005^2$. Assuming a moderate flow rate of $\bar{v}\sim 5$ cm s$^{-1}$, we have $r\sim 10^{18}$ s$^{-1}$. For a typical optical regime, $\omega\sim 10^{15}$ s$^{-1}$, we have a power of about 4 W, enough to run electrical gadgets like clocks and radio. Note that the power is proportional to the flow rate $r$, which depends on the mean velocity of the particles in the guiding tube.

## IV. THERMODYNAMIC ANALYSIS

The thermodynamics of the heat converter in Fig. 1(a) can be analyzed by referring to the heat engine schematic depicted in Fig. 1(b).

### A. Heat engine

The total heat energy (per particle) from the heat source (at higher temperature $T_H$) is

$$Q_H=\tfrac{3}{2}k_BT_H+p_H\hbar\omega, \tag{14}$$

composed of the internal energy $Q_{H,\mathrm{int}}=p_Hr\hbar\omega$, which is only due to the excited population $p_a=p_H=\frac{1}{1+\exp(x)}$, $x=\hbar\omega/k_BT_H$, and the external $Q_{H,\mathrm{ext}}=\frac{3}{2}k_BT_H$ energy, which is obtained from the kinetic theory and the equipartition theorem.

The power of the maser-laser photons is $\frac{d}{dt}\bar{W}_{\mathrm{pho}}=P=p_H\frac{dN}{dt}\rho_{bb}(\tau)\hbar\omega$, where we have used $P\approx\rho_{bb}(\tau)r\hbar\omega$ and $r=p_H\frac{dN}{dt}$, which is less than the rate of particles flowing into the Stern-Gerlach device, $\frac{dN}{dt}$. Thus, the laser work per particle is

$$W_{\mathrm{pho}}=\frac{d\bar{W}_{\mathrm{pho}}}{dt}\Big/\frac{dN}{dt}=p_H\rho_{bb}(\tau)\hbar\omega. \tag{15}$$

The exhaust particles exiting the cavity serves as a heat sink (at lower temperature $T_L$), satisfying the detailed energy balance with the total heat (per particle) $Q_L = Q_H - W_{\rm pho}$, or

$$Q_L = \tfrac{3}{2}k_B T_H + p_H \hbar\omega - W_{\rm pho}, \tag{16}$$

which is due to the kinetic energy $Q_{L,\rm ext} = \frac{3}{2}k_B T_H$ and the internal energy not converted into lasing photons but carried by the exiting particles in the excited state, $Q_{L,\rm int} = (p_H\hbar\omega - W_{\rm pho}) = p_H \rho_{aa}(\tau)\hbar\omega$.

For a large transit time $\tau$ the particle exits the laser cavity with equal probability in the ground state $|b\rangle$ and the excited state $|a\rangle$. This means that only half of the internal energy ($\frac{1}{2}Q_{H,\rm int}$) goes to the lasing photons. The remaining exhaust energy $\frac{3}{2}k_B T_H + \frac{1}{2}p_H\hbar\omega$ becomes the heat sink that is recycled back through the hot reservoir [see Fig. 1(b)].

The internal degree and the external degree (kinetic energy) of the exhaust particles thermalize through inelastic collisions on the way back to the hot reservoir, resulting in a lower temperature $T_L$ that satisfies

$$\tfrac{3}{2}k_B T_H + \rho_{aa}(\tau)p_H\hbar\omega = \tfrac{3}{2}k_B T_L + p_L\hbar\omega, \tag{17}$$

where $p_L = \frac{1}{1+\exp(y)}$ and $y = \hbar\omega/k_B T_L$.

The consideration of thermalization provides the heat sink temperature $T_L$ which is necessary for us to study the thermodynamics of the system. Otherwise, nonequilibrium processes do not allow us to define the temperature $T_L$ for establishing an analogy with the standard thermodynamic heat engine.

Figure 5(a) shows that $T_L < T_H$ and it varies almost linearly with $T_H$. The exhausted particles serve as a heat sink at temperature $T_L$, with a finite (nonzero) energy $Q_L$ after some of its input energy $Q_H$ has been converted to work. Thus, the heat converter setup is a typical heat engine that runs between two different temperatures, where energy flows from the reservoir at $T_H$ to the reservoir at a lower temperature $T_L$. The rejected heat $Q_L = \frac{3}{2}k_B T_H + \rho_{aa}(\tau)p_H\hbar\omega$ in the exhaust fluid is topped up by an amount $W_{\rm pho} = \rho_{bb}(\tau)p_H\hbar\omega$ after passing through the heat source, to be reused for the next cycle.

The presence of rejected or exhaust heat $Q_L$ as a byproduct at lower temperature $T_L$, the work $W_{\rm pho}$ delivered through the laser photons, and the reservoirs with two temperatures

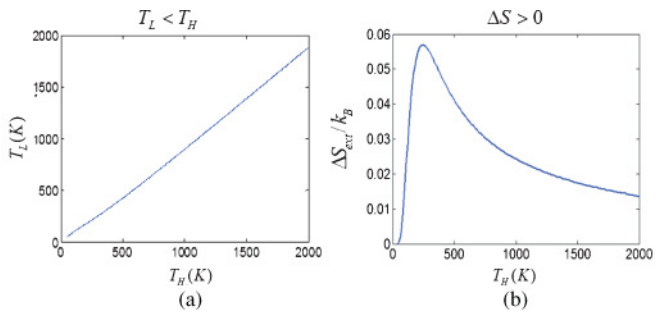


FIG. 5. (Color online) (a) Thermalized temperature $T_L$ of the particles as a heat sink. (b) Entropy change in a cycle (essentially due to external entropy), $\Delta S = (Q_{L,\rm ext} - Q_{H,\rm ext})/T_L + W_{\rm pho}/T_H$ created after the thermalization and passing through the heat source, in agreement with the second law.

$T_L$ and $T_H$ clearly show that the setup in Fig. 1(a) is not a perpetual motion machine of the second kind (PMM2). The setup does not run on a single-temperature reservoir, and it does not convert the entire input energy $Q_H$ to work $W_{\rm pho}$. If no work were delivered, the temperature of the exhaust particles would be unchanged (remaining at $T_H$). A single reservoir that does not do work is not a PMM2. The particles in a single temperature reservoir would also not be able to extract any net heat from the hot reservoir when passing through it. Before we can connect our analysis with the second law, the internal entropy change has to be computed correctly. Note that the internal entropy may *not* be defined like the external entropy by writing $S_{L,\rm int}/k_B = Q_{L,\rm int}/T_L = \frac{y}{1+\exp(y)}$ and $S_{H,\rm int}/k_B = Q_{H,\rm int}/T_H = \frac{x}{1+\exp(x)}$. Proper expressions for the internal entropy are obtained from the quantum von Neumann entropy, as discussed in detail in Sec. V.

### B. Efficiency

If only the internal energy is considered as the input energy (i.e., we neglect the external energy due to the center-of-mass motion), the input power is $\dot{Q}_{\rm int} = p_H r\hbar\omega$ ($p_H = \frac{1}{1+\exp(x)}$, $x = \hbar\omega/k_B T_H$) and the (internal) efficiency $\eta_{{\rm int},a}(\tau) = W_{\rm pho}(\tau)/Q_{{\rm int},H} = p_H\rho_{bb}(\tau)\hbar\omega/p_H\hbar\omega = \rho_{bb}(\tau)$ is determined by the population of the particles exiting from the maser-laser cavity, which is 50% for above-threshold laser operation. The overall efficiency, including the external energy, is

$$\eta(\tau) = \frac{W_{\rm pho}(\tau)}{Q_{\rm ext} + Q_{\rm int}} = \rho_{bb}(\tau)\frac{2x}{3 + 3e^x + 2x}, \tag{18}$$

which has a maximum of 7.83% when $x = \hbar\omega/k_B T_H \simeq 1.28$ for $\rho_{bb}(\tau) = 1/2$. The low efficiency of the heat converter is not a concern since the input energy source is a heat reservoir such as the "ever-present" heat from the ambience or the sun, which can be acquired for free.

The external entropies of the two reservoirs are $S_{H,\rm ext} = Q_{H,\rm ext}/T_H$ and $S_{L,\rm ext} = Q_{L,\rm ext}/T_L$, respectively. Thus, the external entropy difference between the two heat reservoirs is $S_{L,\rm ext} - S_{H,\rm ext} = \frac{3}{2}k_B - \frac{3}{2}k_B = 0$. This result, together with $Q_{L,\rm ext} + Q_{L,\rm int} = Q_{H,\rm ext} + Q_{H,\rm ext} - W_{\rm pho}$, is used to derive an alternate expression for the efficiency that relates to $\eta_c = 1 - \frac{T_L}{T_H}$, the Carnot efficiency, as

$$\eta = \frac{W_{\rm pho}}{Q_H} = \frac{\eta_c + \frac{2}{3}x(p_H - p_L)}{\frac{2}{3}xp_H + 1}, \tag{19}$$

which corresponds to Eq. (19). Note that $p_L - p_H$ is negative for $T_H$ below certain value, called $T_X$. That means that at $T_X$ we have the maximum efficiency $\eta = \frac{\eta_c}{\frac{2}{3}xp_H+1}$.

The friction between the fluid and the confining surfaces or guiding tube prevents continuous motion of the fluid. Frictionless flow or persistent flow is not possible. Thus, a small amount of energy (taken from the laser) is needed to drive the flow of the fluid (see the driver in Fig. 1). By using a guiding tube which can minimize inelastic collisions between the confining surface and the particles, the power needed to drive the quantum fluid in one direction is estimated to be

$$W_{\circlearrowleft} = \bar{v}F = \bar{v}\mathcal{P}A, \tag{20}$$

where $\mathcal{P}$ is the fluid pressure. For $\bar{v} \sim 5$ cm s$^{-1}$, $\mathcal{P} = 10^5$ Pa, and $A = \pi 0.005^2$ we have $W_{\circlearrowleft} = 0.4$ W, which is much less than the output laser power of 4 W obtained above.

Thus, the net work is $W_{\rm net}(\tau) = W_{\rm pho}(\tau) - W_{\rightarrow}$ and the net efficiency is

$$\eta_{\rm net}(\tau) = \frac{W_{\rm net}(\tau)}{Q_{\rm ext} + Q_{\rm int}} = 2x\frac{\rho_{bb}(\tau) - \frac{\mathcal{P}}{\hbar\omega\rho}(1+e^x)}{3+3e^x+2x}, \qquad (21)$$

which is lower than $\eta(\tau)$, where we have used $r = \rho A\bar{v}$.

## V. QUANTUM ENTROPY ANALYSIS

The use of internal states in the scheme reflects the quantum nature of the process. The SG separation enables us to identify an internal state via its path and then manipulate the appropriate ensemble. Initially, the internal state is $\hat{\rho}_i = (p_a|a\rangle\langle a| + p_b|b\rangle\langle b|)|h\rangle\langle h|$. The proper description of the internal entropy is the von Neumann entropy

$$S_i/k_B = S_a + S_b = -p_a \ln p_a - p_b \ln p_b, \qquad (22)$$

which has an upper limit of $\ln 2 \simeq 0.693$ when $p_a = 0.5$.

After the SG device, the internal degree becomes "entangled" with the path, $\hat{\rho}_{SG} = p_a|a\rangle_{UU}\langle a| + p_b|b\rangle_{LL}\langle b|$. There is an uncertainty of finding the particle due to the existence of two [upper ($U$) and lower ($L$)] paths, which introduces spatial distinguishability to the entropy $S_{SG}/k_B = S_U + S_L = -p_a \ln p_a - p_b \ln p_b$, which is the same as the initial entropy since the SG process is unitary and no dissipative mechanism was involved. Thus, the total entropy is unchanged and the second law is not violated. Suppose we try to detect a particle after the SG stage. If the populations are equal, the uncertainty of finding the particle is maximum. If all particles are in a single state, we know in which path the atom can be found and $S_{SG} = 0$.

The overall state of the particles after exiting the cavity is $\hat{\rho}_{\rm cav}(\tau) = p_a\rho_{aa}(\tau)|a\rangle_{UU}\langle a| + p_a\rho_{bb}(\tau)|b\rangle_{UU}\langle b| + p_b|b\rangle_{LL}\langle b|$. It seems that the internal entropy decreases, violating the second law. The key point to resolving the paradox here is that the states $|b\rangle_L$ and $|b\rangle_U$ are distinguishable. The corresponding internal entropy should be

$$S_{\rm cav}(\tau)/k_B = -p_a\rho_{aa}(\tau)\ln p_a\rho_{aa}(\tau) - p_a\rho_{bb}(\tau)\ln p_a\rho_{bb}(\tau) - p_b \ln p_b. \qquad (23)$$

Looking at only the exiting particles in the upper path, we find that the internal entropy is

$$S^u_{\rm cav}(\tau)/k_B = -\rho_{aa}(\tau)\ln\rho_{aa}(\tau) - \rho_{bb}(\tau)\ln\rho_{bb}(\tau), \qquad (24)$$

where $\rho_{bb}(\tau) + \rho_{aa}(\tau) = 1$. The internal entropy of the particles exiting the maser cavity is finite because there is a finite probability to be in both the excited and lower levels. For large $\tau$ we have $\rho^{(m)}_{aa}(\tau) = \rho^{(m)}_{bb}(\tau) = 0.5$, and thus $S^u_{\rm cav}(\tau)/k_B = \ln 2$. In the laser case, Fig. 4(b) shows that the internal entropy in the upper path vanishes, $S^u_{\rm cav} \to 0$, since $\rho_{aa}(\tau) = 1$ for large $\tau$. Since $S^u_{\rm cav}$ is only the entropy of a subsystem (upper path), this should not be mistaken as a violation of the second law.

We should use the overall internal entropy $S_{\rm cav}$ as given by Eq. (23). Then, we find the that second law is *not* violated. Note that if we do not distinguish between the upper and lower paths, or the states $|b\rangle_U$ and $|b\rangle_L$, we might incorrectly interpret Eq. (24) as the internal entropy and find that the internal entropy of all the particles in both paths is reduced by the *selective stimulated emissions* process, violating the second law. In fact, the process does not reduce the internal entropy and neither does it discard the internal entropy into the external entropy of the center-of-mass subsystem since there is essentially no change in the center-of-mass entropy during the stimulated emission. This process is different from the coherent optical processes driven by lasers where the entropy of a subsystem can be reduced at the expense of increasing the entropy of another subsystem [8].

## VI. ENTROPY CHANGE AND THE SECOND LAW

Based on the above quantum entropy analysis for the initial internal entropy of Eq. (22) and the internal entropy after exiting the laser cavity, Eq. (23), we have the internal entropy change

$$(S_{\rm cav} - S_i)/k_B = -p_a\{\rho_{aa}(\tau)\ln\rho_{aa}(\tau) + \rho_{bb}(\tau)\ln\rho_{bb}(\tau)\}, \qquad (25)$$

which is between 0 and $\frac{1}{2}\ln 2 \simeq 0.35$ for $p_a = 0.5$.

After the beam combination, $S_{\rm comb}/k_B = -p'_a \ln p'_a - p'_b \ln p'_b$, where $p'_a = p_a\rho_{aa}(\tau)$ and $p'_b = p_b + p_a\rho_{bb}(\tau)$. The internal entropy decreases due to the reduction in the number of paths. This is compensated by the increase in the center-of-mass entropy $\delta S_{cm} (> |\Delta S_{\rm comb}|)$ by at least the same amount as discussed in Sec. II C. There is also a slight broadening ($\sim \hbar k$) in the momentum distribution of the particles as a result of particle recoil [22] but the contribution is negligible.

After thermalization, the internal entropy becomes $S_{\rm thm}(\tau)/k_B = -p_L \ln p_L - (1-p_L)\ln(1-p_L)$, which is less than $S_i$. In the heat source, the internal entropy increases, back to $S_i$. In each cycle, the total internal entropy change is zero: $\Delta S_{\rm int} = (S_i - S_{\rm thm}) + (S_{\rm thm} - S_{\rm comb}) + (S_{\rm comb} - S_{\rm cav}) + (S_{\rm cav} - S_i) = 0$.

However, the total external entropy change $\Delta S_{\rm ext} = \Delta S^{\rm source}_{\rm ext} + \Delta S^{\rm sink}_{\rm ext}$ is due to the change in the heat sink (during thermalization), $\Delta S^{\rm sink}_{\rm ext} = (Q_{L,\rm ext} - Q_{H,\rm ext})/T_L$, and the change inside the heat source, $\Delta S^{\rm source}_{\rm ext} = W_{\rm pho}/T_H$. Thus, we have

$$\Delta S_{\rm ext} = \frac{W_{\rm pho}}{T_H} - \frac{Q_{H.\rm ext} - Q_{L,\rm ext}}{T_L} = k_B\left[\rho_{bb}(\tau)xp_H - \frac{T_H}{T_L} + 1\right]. \qquad (26)$$

Since the external entropy change is positive, as shown in Fig. 5(b), the total entropy change is positive. Therefore, the second law is satisfied.

The entropy change may also include other sources such as the entropy of the laser photons, $S_{\rm pho}/k_B = -\sum_n \rho_{nn}\ln\rho_{nn}$, associated with the finite width of the photon number distribution in the maser-laser field. For a laser with a Poissonian distribution [Eq. (10)] the photon entropy is

$$S_{{\rm pho},c}/k_B = e^{-\langle n\rangle_c}\sum_{n=0}\frac{\langle n\rangle^n_c}{n!}[\ln n! - n\ln\langle n\rangle_c + \langle n\rangle_c]. \qquad (27)$$

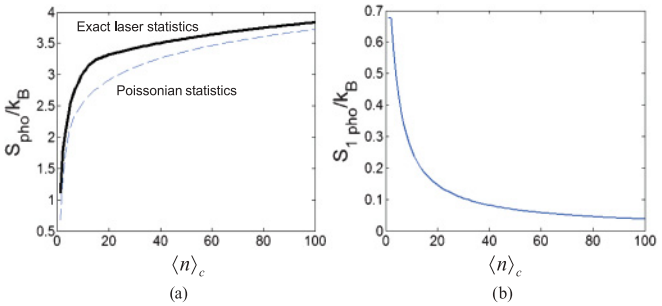


FIG. 6. (Color online) (a) Photon entropy $S_{\rm pho}$ versus mean photon number for the coherent state $\langle n\rangle_c$ of a laser with exact photon statistics (thick solid line) and Poissonian statistics (thin dashed line). (b) Entropy of a single photon, $S_{1\rm pho} = S_{\rm pho}/\langle n\rangle$, reduces with $\langle n\rangle_c$.

Figure 6(a) shows that the laser photon entropy increases with $\langle n\rangle_c$ (but more slowly for larger $\langle n\rangle_c$) for a Poissonian distribution and the exact photon statistics of Eq. (7) with $\bar{n}_{th} = 0$. The photon entropy is independent of $T_H$. The entropy of one photon associated with one particle can be obtained by dividing by $\langle n\rangle$, $S_{1\rm pho} = S_{\rm pho}/\langle n\rangle$. We find that $S_{1\rm pho} \to 0$ for large $\langle n\rangle$ as shown in Fig. 6(b).

Thus, the inclusion of the laser photon entropy along with the center-of-mass and internal entropies gives $\Delta S = \Delta S_I + \Delta S_{\rm ext} + S_{1\rm pho} + \delta S_{cm}$, which is obviously positive, in agreement with the second law.

## VII. CONCLUSIONS

We have analyzed the scheme that can convert thermal energy from any heat source to useful energy in the form of maser-laser light. This scheme uses a Stern-Gerlach device and a maser-laser cavity (stimulated emission process) to extract the photon energy from the internal degree of the excited particles. Analysis of the internal dynamics of the particles and photon statistics provides insights into the physical conditions for optimizing the output of photons. The energy efficiency of the system has been estimated. The proposed setup is a heat engine which runs on two heat reservoirs with different temperatures while producing laser work. The engine is a generalization of the classical heat engine with the inclusion of the change in the internal energy due to variable populations of the quantum states. Thermodynamic analysis shows that the setup is not a perpetual motion machine of the second kind. The total change in the internal and external entropies for each cycle always increases. Thus, the cyclic process does not violate the second law of thermodynamics and the heat converter is feasible. The scheme may run on any heat source, for example natural heat source from the sun or geothermal sites that provide green and renewable energy.

## ACKNOWLEDGMENTS

This work is supported by University Malaya HIR Grant No. J-00000-73588 and the Ministry of Higher Education FRGS Grant No. FP005/2010B. The author is grateful to M. O. Scully and P. R. Berman for stimulating discussions.

[1] For illuminating discussions on the second law and quantum thermodynamics, see the recent text by E. P. Gyftopoulos and G. P. Beretta, *Thermodynamics. Foundations and Applications* (Dover, New York, 2005), which generalizes and improves its more famous predecessor, G. N. Hatsopoulos and J. H. Keenan, *Principles of General Thermodynamics* (Wiley, New York, 1965).

[2] *Meeting the Entropy Challenge, An International Thermodynamics Symposium*, edited by G. P. Beretta, A. F. Ghoniem, and G. N. Hatsopoulos, AIP Conf. Proc. **1033** (2008).

[3] W. Ketterle and D. E. Pritchard, Phys. Rev. A **46**, 4051 (1992).

[4] H. S. Leff and A. F. Rex, eds., *Maxwell's Demon: Entropy, Information, Computing* (Princeton University Press, Princeton, 1990).

[5] S. Lloyd, Phys. Rev. A **56**, 3374 (1997).

[6] E. Schrödinger, *What is Life?: The Physical Aspect of the Living Cell* (Cambridge University Press, New York, 1992).

[7] M. O. Scully, Phys. Rev. Lett. **87**, 220601 (2001).

[8] C. H. R. Ooi, K.-P. Marzlin, and J. Audretsch, Eur. Phys. J. D **22**, 259 (2003).

[9] B. Friedrich and D. Herschbach, Phys. Today **56**, 53 (2003). This review paper gives the historical achievement of Otto Stern and Walther Gerlach who used hot (1000 °C) Ag atoms with a magnet of length 3.5 cm, strength 0.1 T, and gradient of 10 T/cm, which led to a beam separation of about 0.2 mm.

[10] J. P. Gordon, H. J. Zeiger, and C. H. Townes, Phys. Rev. **99**, 1264 (1955).

[11] M. Sargent, M. Scully, and W. Lamb, *Laser Physics* (Addison-Wesley, Reading, MA, 1974).

[12] R. Feynman, R. Leighton, and M. Sands, *The Feynman Lectures on Physics*, Vol. 3 (Addison-Wesley, Palo Alto, CA 1966), Sec. 9.

[13] M. O. Scully, Phys. Rev. Lett. **88**, 050602 (2002).

[14] G. P. Beretta, e-print arXiv:quant-ph/0703261.

[15] A. Browaeys, A. Robert, O. Sirjean, J. Poupard, S. Nowak, D. Boiron, C. I. Westbrook, and A. Aspect, Phys. Rev. A **64**, 034703 (2001).

[16] The complication may be surpassed by using diatomic molecules with very few Franck-Condon branching factors.

[17] P. Filipowicz, J. Javanainen, and P. Meystre, Phys. Rev. A **34**, 3077 (1986).

[18] M. O. Scully, Phys. Rev. Lett. **16**, 853 (1966).

[19] V. I. Klimov, Science **290**, 314 (2000).

[20] N. Lu, and J. A. Bergou, Phys. Rev. A **40**, 237 (1989).

[21] M. O. Scully, Y. Rostovtsev, Z. E. Sariyanni, and M. S. Zubairy, Physica E **29**, 29 (2005).

[22] C. H. R. Ooi, K.-P. Marzlin, and J. Audretsch, Phys. Rev. A **66**, 063413 (2002).